HTML ABSTRACT + LINKS

APPLIED PHYSICS LETTERS VOLUME 85, NUMBER 10 6 SEPTEMBER 2004

Deep subsurface electronic defect image contrast and resolution amplification in Si wafers using infrared photocarrier radiometry

Jerias Batista,[a] Andreas Mandelis, Derrick Shaughnessy, and Bincheng Li
Center for Advanced Diffusion-Wave Technologies (CADIFT), Department of Mechanical and Industrial Engineering, University of Toronto, Toronto M5S 3G8, Canada

(Received 15 December 2003; accepted 1 July 2004)

A photocarrier radiometry technique using a secondary subband-gap dc light source is introduced, along with the applications to deep subsurface electronic defect analysis in Si wafers. It is shown that the use of a dc light source, in addition to the modulated laser beam, drastically enhances the potential of the technique in resolving low-level damage otherwise virtually indistinguishable by conventional photothermal techniques. Using this methodology, the overall contrast enhancement was about 386% for amplitude and 5586% in phase over conventional photocarrier radiometry. © *2004 American Institute of Physics*. [DOI: 10.1063/1.1785289]

Bulk lifetime and surface recombination velocity are the most commonly used parameters for detection and characterization of defects in Si wafers, particularly those induced by metallic contamination.[1–4] Several different methods have been developed to monitor either absolute values of minority carrier lifetime and surface recombination velocity or their relative changes induced by the presence of defects. These methods usually consist of the injection of excess carriers and the measurement of some quantity related to the free carrier dynamics. For instance, the surface photovoltage method measures the bending of the energy bands (or surface potential) upon illumination;[4] the photoconductance method measures the intensity decay of a microwave due to changes in the IR absorption coefficient after cessation of the excitation;[5] the ELYMAT technique measures the photocurrent collected by a semiconductor–metal contact;[6] and, lately, infrared photocarrier radiometry selectively measures the infrared emission from free photoexcited carrier-density waves (CDW).[7–9]

Infrared photocarrier radiometry (PCR) was recently introduced as a noncontact methodology to study electronic transport properties in semiconductor materials. The physical principles of the PCR method, a form of spectrally gated near-infrared room-temperature photoluminescence emission, were presented by Mandelis *et al.*,[7] along with the experimental evidence of its potential for semiconductor analysis. Briefly, in a photoexcited semiconductor of band-gap energy E_G, an intensity-modulated incident optical source such as a laser beam (in the present case, a diode laser, $\lambda_{ac} = 830$ nm; $P_{ac} = 30$ mW; beam radius on the sample: 0.066 mm) with superband-gap energy photons $\hbar\omega > E_g$, is absorbed and generates a CDW.[9] Following several pathways, the free carriers will diffuse in their respective energy bands until they recombine across the band gap or into impurity and/or defect states within the band gap. The reestablishment of the free carrier equilibrium is accompanied by emission of phonons, thus raising the temperature locally (thermal nonradiative component), as well as by emission of photons of near- or subband-gap energy (direct emission component). The distance $L_{ac}^{j} = L_{dc}^{j}/(1+i\omega\tau_j)^{1/2}$ that the CDW travels before recombination, which is experimentally controlled through the modulation frequency f of the laser beam, is the ac carrier diffusion length, a critical parameter for semiconductor analysis, as it depends on the carrier lifetime τ_j, a physical parameter strongly sensitive to defects or impurities. Here, $L_{dc}^{j} = (D_j^{*}\tau_j)^{1/2}$ stands for dc diffusion length, D_j^{*} is the ambipolar diffusion coefficient and $j=n$ (electrons) or $j=p$ (holes). In the conventional PCR setup, a room-temperature InGaAs detector (0.8–1.8 μm bandwidth) with integrated amplification electronics and spectrally gated optical filters to match the detector bandwidth is used instead of the liquid-nitrogen-cooled HgCdTe photodetector (2–12 μm bandwidth) used in conventional photothermal radiometry.[10] The major advantage of this technique over other photothermal techniques, such as photomodulated thermoreflectance[11] and infrared radiometry, lies in its ability to study purely electronic carrier-wave recombination kinetics with no thermal-wave interference from synchronous Planck-mediated infrared emissions due to the concurrent lattice absorption of the incident laser beam and nonradiative heating. In the case of PCR with secondary light, an unmodulated (dc) IR laser (diode laser, $\lambda_{dc} = 1500$ nm; $P_{dc} = 4$ mW; beam radius on the sample: 1 mm) is coincident with, and fully overlaps, the modulated laser spot. Both lasers are incident on the same polished side of the wafer, which in this case was supported by a polished aluminum holder.

In this letter, we report an application of the PCR technique using a secondary subband-gap dc light source. It is shown that the combination of PCR and dc light enhances drastically the potential of PCR in resolving low-contrast features otherwise virtually impossible to detect using photothermal techniques. A complete theory of PCR with secondary dc light is currently under development. Here, we will concentrate on the basic physical principles of the signal generation and on the discussion of some experimental results to demonstrate the potential of the methodology as an electronic feature imaging resolution amplifier.

The physics of the contrast mechanism for the nonthermal nature of the PCR signal is based on the self-absorption of recombination-generated IR photons emitted by the photoexcited CDW distribution throughout the wafer bulk.[7] The distribution profile is modified by enhanced recombination at

[a]On leave from: Departamento de Física, Universidade Federal do Maranhão, São Luís, MA, Brazil; electronic mail: jbatista@ufma.br

Reuse of AIP Publishing content is subject to the terms at: https://publishing.aip.org/authors/rights-and-permissions. Download to IP: 128.100.49.199 On: Fri, 18 Mar 2016 01:22:57

 © 2004 American Institute of Physics

localized or extended defects either at the wafer surface or inside the bulk. The addition of an IR dc light source with spectral content within the detector bandwidth of the PCR instrument amplifies signal contrast as follows: The almost transparent semiconductor to the subband-gap radiation acts as a lossy multipass medium for the subband-gap radiation, the latter being multiply reflected by the front and back surfaces of the sample and controlled by the effective reflectivity of the combined back surface and IR-reflecting support. The loss factor is controlled by the modulated superband-gap laser source-induced infrared absorption/emission depth profile (in the sense of the Detailed Balance Principle).[7] This in turn cross modulates the intensity of the dc radiation which is superposed on the direct back-propagated emission signal from recombining carriers and is synchronously detected by the PCR detector. Strong enhancement of recombination features that contribute to the IR CDW absorption/emission coefficient distribution profile across the sample (and its spectral integral at the detector) occurs by virtue of the multipass (at least double-pass) attenuation of the back-propagated IR radiation which thus acts as an amplifier of the absorption/emission profile within the ac CDW diffusion length and integrated over the thickness of the sample.

Direct emission occurs only from de-excitation of the CDW, so that the IR absorption coefficient is highest when the ac laser is on. This component of the synchronous signal can be called "in phase". During the part of the cycle when the modulated laser is off, the IR absorption coefficient is lowest. This amounts to the semiconductor attaining the minimally lossy state, as far as the multipass dc radiation is concerned, and maximum transmission of the cross-modulated intensity occurs which dominates the back-propagated signal. Because of its timing within the modulation cycle, this component of the synchronous signal can be called "out of phase" and it clearly lags the direct PCR signal component by 180°, assuming instantaneous relaxation of all recombination processes (generally valid at low modulation frequencies such that $\omega\tau_j \ll 1$). Depending on the intensity of the dc IR laser beam, the combined PCR amplitude ranges from some value dominated by pure PCR (dc laser off) to some other value, usually higher, which is transmittance dominated. For some intermediate dc laser intensity, the combined PCR signal reaches a minimum explained by the vectorial interplay between the in-phase and out-of-phase components. In the case where $\omega\tau_j \gg 1$, an additional phase shift due to the finite relaxation rate of the carrier-wave will broaden the phase, so that the combined phase will be a function of the carrier lifetime (ranging between 0 and 90°).[7] Therefore, the maximum phase shift allowed for the combined PCR signal between fully in-phase recombination, $\omega\tau_j \ll 1$, and fully delayed, $\omega\tau_j \gg 1$, recombination is 270°. A similar behavior was observed by Dietzel *et al.*[12] in their broadband IR transmittance experiment, using conventional photothermal radiometry and a HgCdTe detector in the pump–probe configuration. In that case, a heater at 650 K was used as an IR probe emitter, and the wafer was placed in between the heater and the detector. The intrinsic disadvantage of this configuration comes from the fact that the secondary IR source is a broadband Planck emitter, which peaks around 4 μm, involving the thermal infrared contributions to the radiometric signal and complicating data analysis, albeit to a lesser extent than conventional photothermal radiometry.

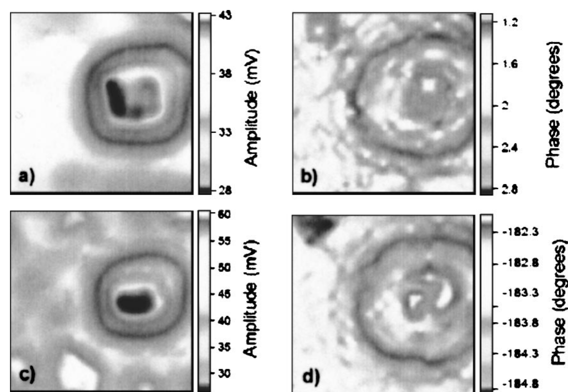

FIG. 1. PCR amplitude and phase maps obtained by scanning an area 5×5 mm^2 from the front side of a Si wafer with a defect on the back side. (a,b) Amplitude (phase) with dc IR laser off. (c,d) Amplitude (phase) with dc IR laser on. Experimental parameters: $\lambda_{ac}=830$ nm, $P_{ac}=30$ mW; spot size=0.132 mm, $f=100$ Hz. $\lambda_{dc}=1500$ nm, $P_{dc}=4$ mW; spot size: 2 mm. Number of data points: 400.

To show the resolution amplification of PCR by using a secondary dc IR laser source, a small area of the back surface of a *p*-type Si wafer (resistivity $\rho\sim20\ \Omega$ cm, 0.675 mm thickness) was very slightly damaged through gentle rubbing with a folded optical paper. The measurements were performed from the front side of the wafer. The actual size of the defect is about 1.8 mm. Figure 1 shows amplitude and phase images with the dc laser off [Figs. 1(a) and 1(b)] and with the dc laser on [Figs. 1(c) and 1(d)]. The ac laser was modulated at 100 Hz. The scanned area was 5×5 mm^2, and 400 data points were measured for each image. In both configurations, the localization and geometry of the defect is clearly seen. This particular wafer was measured[7] to have $\tau_j\cong1$ ms and $D^*\cong12$ cm^2/s, which yields an $|L_{ac}|\cong1$ mm. Therefore, the carrier-wave centroid lies well beyond the thickness of the wafer and only a small phase shift can be observed with the dc laser off. However, the cross-modulated component of the IR laser produced an amplified phase contrast (see below). Figure 2 shows the same set of measurements performed at 100 kHz. At this frequency, the ac carrier diffusion length $|L_{ac}|$ is only 0.044 mm, and despite the fact that the ac carrier-wave centroid lies very far from the defect, the PCR amplitude still shows contrast [Fig. 2(a)], accompanied by a very small phase shift [Fig. 2(b)]. Nevertheless, the

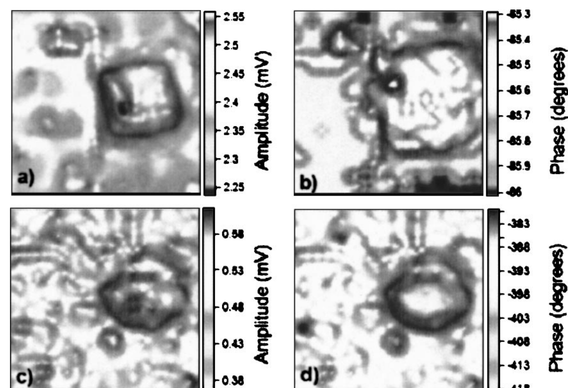

FIG. 2. PCR amplitude and phase maps obtained by scanning an area 5×5 mm^2 from the front side of a Si wafer with the defect on the back side. (a,b) Amplitude (phase) with dc IR laser off. (c,d) Amplitude (phase) with dc IR laser on. The experimental parameters were the same as in Fig. 1, but $f=100$ kHz.

Reuse of AIP Publishing content is subject to the terms at: https://publishing.aip.org/authors/rights-and-permissions. Download to IP: 128.100.49.199 On: Fri, 18 Mar 2016 01:22:57

presence of the IR laser increased drastically the contrast for both amplitude [Fig. 2(c)] and phase [Fig. 2(d)] channels, as a result of a diminished direct (in-phase) PCR component compared to the out-of-phase multipass contribution. Defining contrast as $C=(S_{\max}-S_{\min})/(S_{\max}+S_{\min})$, we see that the contrast of the PCR amplitude at 100 Hz was about 21.8% (dc off) and 39% (dc on), and that the phase difference was 1.75° (dc off) and 3° (dc on). The relative contrast enhancement was about 179% in amplitude and 171% in phase. It is worth noting that the condition $\omega\tau_j \ll 1$ is fulfilled, so that the PCR phase with the dc laser off (in phase) is close to 0°, and with the dc laser on (out of phase) is close to −180°. In the latter case, the transmission component dominates the PCR signal, as expected. Some subtler features appear, especially in the phase image, which were otherwise invisible without the dc light. At 100 kHz, the contrast of the PCR amplitude was 6.67% (dc off) and 25.77% (dc on), and the phase difference was 0.7° (dc off) and 39.1° (dc on). The relative contrast enhancement was 386% for amplitude and 5586% in phase. At this frequency, the condition $\omega\tau_j \ll 1$ is not fulfilled; consequently, the maximum combined phase shift between $\omega\tau_j \ll 1$ and $\omega\tau_j \gg 1$ conditions, for this particular IR cross-modulated intensity, was 233° [see Figs. 1(d) and 2(d)].

One advantage of this contrast amplification methodology comes from the fact that the contrast between good and defective regions of the wafer can be controlled, at least in principle, by controlling the intensity of the secondary dc light. During the measurements, the dc IR laser power was kept constant. However, the increase of the back-surface recombination velocity decreased the free-carrier density near the defect, thus decreasing the infrared absorption coefficient. As a result, the transmitted component of the IR multipass laser increased, and so did the image contrast. It is important to mention that neither conventional PCR (dc IR laser off) nor transmission techniques are able to produce image contrasts as large as 180°. Measurements performed from the back side of the wafer (crossing the defective area) and not shown here, exhibited phase contrast of about 168° with the dc IR multipass laser on, while the contrast was only 27° without it. Another very important advantage of this methodology concerns the image distortion of the defective area. With regard to the fidelity of images obtained by CDW techniques, one has to proceed with care, as the probing ac CDW diffusion length has to be taken into account. At low frequency, both maps for amplitude [Fig. 1(a)] and phase [Fig. 1(b)] with the dc IR laser off appear larger than the actual size of the defect (about 1.8 mm). The reason for this is the large ac CDW diffusion length (about 1 mm at 100 Hz), which allows free carriers generated within this distance from the defect region to diffuse into the defect region and recombine there accompanied by photon emissions, thus contributing to the effective defect structure. Therefore, the resolution and contrast are diffusion limited since any defect within the diffusion length influences the carrier dynamics. With the dc IR laser on, the size of the amplitude image is closer to the defect size dimensions because the effects of enhanced cross-modulated IR transmission caused by the diminished direct recombination emission within the actual defect region increase the relative contribution of the former mechanism to the overall PCR signal. This contribution is non-diffusive and thus not limited by the ac diffusion length. The diminished direct recombination emissions in, and around, the defect region are, of course, diffusion-length-limited. The resulting superposition generates mainly cross-modulated optical transmission images close to the actual size of the defect when the dc beam is on. With the dc beam off only diffusion-limited broadened images are possible. The phase exhibits greater resolution over the actual size of the defect, however, it retains a diminished resolution of the surrounding features. At 100 kHz, the images for both amplitude and phase using the dc IR laser show a much improved delineation of the defect as separate from its surrounding damage region and much better detail and clearer structure of the complexity of the damage than without the dc IR light. With the dc laser off, one would have to compromise the lateral resolution in order to discern deep defects. Nevertheless, the presence of the secondary light source enhances the imaging resolution, with both the amplitude [Fig. 2(c)] and phase [Fig. 2(d)] basically showing a geometric projection of the deep subsurface defect on the front surface of the wafer. Based on the experimental evidence discussed above, there are excellent prospects for PCR with a secondary dc IR light as a high-sensitivity defect-imaging tool for wafer characterization. Work currently under way is examining the application of this contrast amplification method to the industrially relevant case of heavy metal contamination imaging, insofar as the presence of such ions can disturb the carrier-density wave, thus affecting PCR contrast.

The authors wish to acknowledge the continuing support of Materials and Manufacturing Ontario (MMO) and Photo-Thermal Diagnostics, Inc., with a Collaborative Project contract, as well as the Natural Sciences and Engineering Research Council of Canada (NSERC).

[1] D. K. Schroder, *Semiconductor Material and Device Characterization*, 2nd ed. (Wiley-Interscience, New York, 1998).
[2] A. A. Istratov, H. Hieslmair, and E. R. Weber, Appl. Phys. A: Mater. Sci. Process. **70**, 489 (2000).
[3] A. Castaldini, A. Cavallini, A. Poggi, and E. Susi, Mater. Sci. Eng., B **42**, 249 (1996).
[4] L. Kronik and Y. Shapira, Surf. Sci. Rep. **37**, 1 (1999).
[5] G. Citarella, S. von Aichberger, and M. Kunst, Mater. Sci. Eng., B **91**, 224 (2002).
[6] D. Walz, G. Le Carval, J.-P. Joly, and G. Kamarinos, Semicond. Sci. Technol. **10**, 1022 (1995).
[7] A. Mandelis, J. Batista, and D. Shaughnessy, Phys. Rev. B **67**, 205208 (2003).
[8] J. Batista, A. Mandelis, and D. Shaughnessy, Appl. Phys. Lett. **82**, 4077 (2003).
[9] A. Mandelis, *Diffusion-Wave Fields: Mathematical Methods and Green Functions* (Springer, New York, 2001), Chap. 9.
[10] A. Mandelis, Solid-State Electron. **42**, 1 (1998).
[11] J. Batista, A. M. Mansanares, E. C. da Silva, and D. Fournier, J. Appl. Phys. **82**, 423 (1997).
[12] D. Dietzel, J. Gibkes, S. Chotikaprakhan, B. K. Bein, and J. Pelzl, Int. J. Thermophys. **3**, 741 (2003).

Reuse of AIP Publishing content is subject to the terms at: https://publishing.aip.org/authors/rights-and-permissions. Download to IP: 128.100.49.199 On: Fri, 18 Mar 2016 01:22:57